AD-A150 141 ICE STATISTICS AND ACOUSTIC SCATTERING IN THE ARCTIC BASIN(U) SCIENCE APPLICATIONS INTERNATIONAL CORP MCLEAN VA R R GREENE 01 OCT 84 SAIC-84/1132 N00014-84-C-0180 1/1

UNCLASSIFIED F/G 20/1 NL

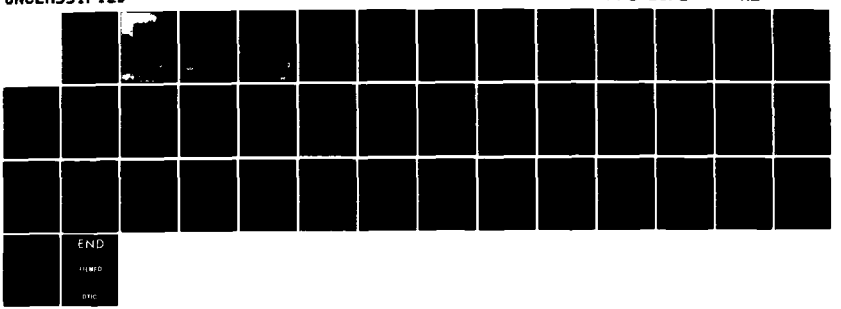

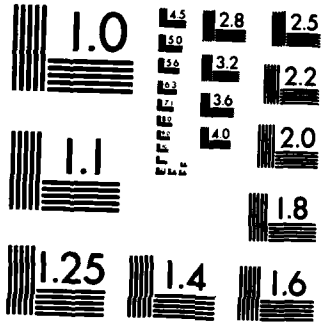

TECHNICAL REPORT
ICE STATISTICS AND ACOUSTIC SCATTERING IN THE ARCTIC BASIN

SAIC-84/1132

SAIC
Science Applications International Corporation

TECHNICAL REPORT
ICE STATISTICS AND ACOUSTIC SCATTERING IN THE ARCTIC BASIN

SAIC-84/1132

SAIC™
Science Applications International Corporation
Post Office Box 1303, 1710 Goodridge Drive, McLean, Virginia 22102, (703) 821-4300

TECHNICAL REPORT
ICE STATISTICS AND ACOUSTIC SCATTERING IN THE ARCTIC BASIN

SAIC-84/1132

October 1984

Prepared
for

Bobby Wheatley
Naval Ocean Research and Development Activity
AEAS Program Office, Code 270
NSTL Station, MS 39529

Prepared
by

Robert R. Greene
Navy Systems Division

Contract No. N00014-84-C-0180

SCIENCE APPLICATIONS INTERNATIONAL CORPORATION

1710 Goodridge Drive
P.O. Box 1303
McLean, Virginia 22102
(703) 821-4300

UNCLASSIFIED

SECURITY CLASSIFICATION OF THIS PAGE (When Data Entered)

REPORT DOCUMENTATION PAGE		READ DISTRUCTIONS BEFORE COMPLETING FORM
1. REPORT NUMBER SAI-84/1132	2. GOVT ACCESSION NO. A150 141	3. RECIPIENT'S CATALOG NUMBER
4. TITLE (and Subtitle) Ice Statistics and Acoustic Scattering in the Arctic Basin		5. TYPE OF REPORT & PERIOD COVERED Technical Report
		6. PERFORMING ORG. REPORT NUMBER SAI-84/1132
7. AUTHOR(s) Robert R. Greene		8. CONTRACT OR GRANT NUMBER(s) N00014-84-C-0180
9. PERFORMING ORGANIZATION NAME AND ADDRESS Science Applications International Corp. 1710 Goodridge Drive McLean, VA 22102		10. PROGRAM ELEMENT, PROJECT, TASK AREA & WORK UNIT NUMBERS Task 27.1, HAPE Applications Task 28.1, Environmental Applications
11. CONTROLLING OFFICE NAME AND ADDRESS NORDA AEAS Program Office Code 270 NSTL, Mississippi 39529		12. REPORT DATE October 1, 1984
		13. NUMBER OF PAGES
14. MONITORING AGENCY NAME & ADDRESS(if different from Controlling Office)		15. SECURITY CLASS. (of this report) Unclassified
		15a. DECLASSIFICATION/DOWNGRADING SCHEDULE

16. DISTRIBUTION STATEMENT (of this Report)

Distribution unlimited

17. DISTRIBUTION STATEMENT (of the abstract entered in Block 20, if different from Report)

18. SUPPLEMENTARY NOTES

19. KEY WORDS (Continue on reverse side if necessary and identify by block number)

Arctic, Acoustic, Scattering, Random, Ice, Ridge, Keel, Statistics, Propagation, Loss

20. ABSTRACT (Continue on reverse side if necessary and identify by block number)

Acoustic reflection loss and transmission loss are calculated based upon statistical models of ice roughness. Statistical models of ice ridging and techniques for estimating the roughness spectra of ridged surfaces are developed.

DD FORM 1 JAN 73 1473 EDITION OF 1 NOV 65 IS OBSOLETE
S/N 0102-LF-014-6601

UNCLASSIFIED

SECURITY CLASSIFICATION OF THIS PAGE (When Data Entered)

TABLE OF CONTENTS

LIST OF FIGURES

INTRODUCTION

Acoustic propagation in the Arctic is intimately related to the structure of surface pack ice. In this paper, reflection loss and transmission loss are calculated based upon statistical models of ice roughness. ~~In Section 1,~~ statistical models of ice ridges are introduced and techniques for estimating the roughness spectrum of ridged surfaces are developed. Next, ~~In Section 2,~~ a model for estimating the mean reflection loss is introduced. The reflection loss formulas are based on the statistical models for roughness ~~introduced~~ in Section 1. ~~In Section 3,~~ transmission loss calculations using High-Angle Parabolic Equation ~~PE~~ (ARCHAPE) in a simulated Arctic environment are compared with data. The results demonstrate that rough surface scattering from random-depth ice keel structures can account for the observed rate of transmission loss in the Arctic. [illegible] include: Acoustic [illegible] Propagation loss.

and

Section 1
DESCRIPTION OF ARCTIC ICE ROUGHNESS

The roughness of the bottom surface of Arctic sea ice has been described using both discrete and continuous statistical models. A discrete model characterizes the under-ice surface as a collection of individual, randomly distributed ice ridge keels. Probability distributions describe individual statistics of the keels such as maximum depth, spacing, and orientation. A discrete model must prescribe a representative ridge shape or an ensemble of ridge shapes, to calculate the statistics of the surface from the discrete statistics of the ice structures. Discrete ice ridge models have been proposed by Diachok[1], Hibler et al.[2,3], Lowry and Wadhams[4], Mock et al.[5], and Wadhams[6]. Continuous statistical models treat the under-ice surface as a stochastic process, and analyze it using techniques familiar from time series analysis. The surface is characterized by its spatial autocorrelation function. Spectral models give a more complete description of the shape of the under-ice surface. However, they are limited in that only surfaces whose depth, h, has a Gaussian distribution can be completely characterized in this way. Spectral models for under-ice roughness have been published by Ackley, et al.[7], Hibler and LeSchack[8], Hibler[9], Rothrock and Thorndike,[10] and Mellen[11]. In the remainder of this section, probability distributions for ridge-keel depth, orientation, and spacing will be developed from first principles, spectral models of the ice surface will be discussed, and techniques for estimating the roughness spectra of discrete models will be developed.

1.1 THE DISTRIBUTION OF DISCRETE ICE STRUCTURES

Ridge-Keel Depth

Using a simple variational derivation, Hibler[2] argues that the cross-sectional area, A, of the deformed ice in an Arctic ice ridge is a random variable with the exponential distribution:

$$1-e^{-aA} \quad . \tag{1}$$

The probability density of the area is obtained by differentiating Eq. (1) with respect to A. It is the familiar exponential density:

$$ae^{-aA} \quad . \tag{2}$$

Hibler's analysis is based on a collection of ridge "links", ice structures of fixed length L, each having a constant but random cross-sectional area. The derivation of the exponential distribution follows intrinsically from Hibler's assumption 2, that given a system of N ridge links of length L, each with cross-sectional area A, "all possible ridge-link (area) arrangements yielding the same net deformation of a given expanse of the ice sheet are equally likely."

Hibler derives a distribution for ridge keel depth based on the assumption that the cross-sectional area, A, is proportional to the square of the depth, h. This is a reasonable assumption if the shapes of the ridge cross-sections are all similar for instance, isosceles triangles with the same base angle).

A Rayleigh distribution for the keel depth,

$$1-e^{-abh^2} , \tag{3}$$

results when the proportionality relation,

$$A=bh^2 , \tag{4}$$

is substituted into Eq. 1. The associated probability density is:

$$2abhe^{-abh^2} . \tag{5}$$

The exponential model for the cross-sectional area is consistent with a negative exponential behavior of mean ice draft for large drafts, a behavior observed by Wadhams[6].

Hibler originally predicted a modified Gaussian distribution for keel depth. This was based on mistakenly substituting Eq. (4) into Eq. (2), in the derivation above. In a later publication, Hibler[3] supports the modified Gaussian distribution as providing a good fit to observed ridge counts. Lowry and Wadhams[4] criticized the Rayleigh distribution, when it was suggested by Diachok[1], as predicting too small a proportion of small ridges. They propose a modification to the Gaussian-type distribution, emphasizing the behavior of the distribution for small ridges. The controversy over the keel depth distribution seems centered on the issue of small ridges.

It will be shown in Section 3 that acoustic transmission loss in the Arctic depends more strongly on the proportion of large ridges. Because the asymptotic behavior of mean ice draft for large drafts supports the Rayleigh

model for large keel depths, the Rayleigh model was chosen for scattering-loss calculations in this report. A modified Rayleigh-type distribution, based on the area proportionality relation:

$$A=bh^2 + ch \ , \tag{6}$$

could be used to improve the behavior for small ridges. The probability density arising from the substitution of Eq. (6) into Eq. (1) is:

$$(2abh + ac)\ e^{-(abh^2 + ach)} \ . \tag{7}$$

1.2 RIDGE ORIENTATION

It is commonly assumed for modeling purposes that ice-ridge orientation is directionally isotropic. This is a reasonable assumption, even though statistical analyses by Mock et al.[5] and Hibler[9] indicate that, locally, there may be a preferred direction for ridge orientation. However, even in the isotropic case, the collection of ridges which intersect a given measurement track are not randomly oriented, but tend to lie perpendicular to the track. The statistics of line segments crossing a given line are discussed by Feller[12], as the Buffon needle problem. It was first mentioned in the context of ice ridge statistics in Mock et al.[5].

The relative probability that a given ridge link of length L will cross the track is proportional to the length of the projection in the direction perpendicular to the track, L sin θ, where θ is the angle between the axis of the ridge and the track. The probability density for the angle of intersection of ridges crossing the track is:

$$(1/2) \sin \theta \, d\theta \quad , \text{ for } 0 < \theta < \pi \, , \tag{10}$$

with the associated distribution function:

$$(1/2) (1 - \cos \theta) \, . \tag{11}$$

1.2.1 Application: Apparent Width of a Ridge

Any linear structure of given width W will appear wider, if it is crossed at an angle. The apparent width is:

$$W_a = W/\sin \theta \, , \tag{12}$$

where θ is the angle of intersection between the axis of the structure and the measurement track. Based upon the distribution of θ given in Eq. (11), W_a has the distribution:

$$\sqrt{(1 - (W/W_a)^2} \text{ on } [W, \infty] \, , \tag{13}$$

and density,

$$W^2/(W_a^2 \sqrt{(W_a^2 - W^2)}) \, dW_a . \tag{14}$$

An immediate consequence is that, in terms of the actual width, W, the mean value of the apparent width is:

$$\langle W_a \rangle = (\pi/2) \, W \, . \tag{15}$$

Eq. (14) can be interpreted as the conditional probability of apparent width for a given actual width:

$$p(W_a|W) \, .$$

1.2.2 Application: The Width Distribution of Leads Along a Track

In Wadhams[6], the number density of leads per kilometer, of observed width d meters, was found to obey a power law:

$$n(d) = 15\ d^{-2}\ . \tag{16}$$

A lead was defined to be a continuous sequence of depth points, greater than 5 meters long and not exceeding 1 meter of draft, as observed from an upward-looking sonar.

A power law like Eq. (16) is easy to distinguish from a negative exponential law. It is easy to devise an argument, however, that the actual width of leads should be exponentially distributed. Leads are formed when tensile forces pull the ice apart. If the ice opens at N parallel leads to a total width of W_t meters, and if all combinations of N lead widths, which sum to W_t, are equally likely, then a negative exponential density for lead width results. The density for actual lead width has the form:

$$p(W) = (1/W_0)\ e^{-W/W_0}\ . \tag{17}$$

The apparent width of randomly oriented leads, as observed along a track, can be obtained by "randomizing" the distribution for actual lead width, Eq. (17), by the conditional distribution for the apparent lead width, Eq. (14), in the form:

$$p(W_a) = \int_0^{W_a} p\ (W_a|W)\ p(W)\ dW\ .$$

This integral can be carried out in closed form, in terms of the special functions I_1, a Bessel function of imaginary argument, and L_1, a modified Struve function, to obtain:

$$(\pi/(2\ W_0))\ [I_1'(W_a/W_0) - L_1'\ (W_a/W_0)]\ . \qquad (18)$$

Asymptotic expansions for these functions reveal that for large argument, $p(W_a)$ is asymptotic to W_a^{-3}. The mean apparent width is:

$$(\pi/2)\ W_0\ ,$$

where W_0 is the actual mean width. Wadhams' distribution for apparent lead width is inversely proportional to the square, rather than the cube, of the width. However, he speculates[6] that in the region where the data was taken, offshore Greenland, the orientation of leads and polynyas may not be isotropic.

1.3 RIDGE SPACING

Ridges appear to be distributed uniformly along measurement tracks, see Hibler[2]. This implies that ridge spacing has a negative exponential distribution. Lowry and Wadhams[4] have published a histogram of observed ridge spacing which departs from the exponential model for spacings below about 100 meters. Since ridges are often indistinguishable when they lie close together, selection rules are used to decide when a structure in the ice consists of one ridge or two. Lowry and Wadhams suggest that the shortage of small ridge spacings in their histogram is an artifact of a selection criterion which counts two close ridges as one. However, to account for the entire deviation their model had to use triangular ridges which are unusually wide for their height.

An alternative explanation for an actual departure from the uniform distribution of ridges along a track can be based on the net expansion of the ice pack due to the ridge formation process. Ridges form in cracks in the ice pack. The spacing between these cracks can be modeled as a random variable with negative exponential distribution. Under tensile forcing the cracks open and are forced partially together again, crushing new ice which has frozen in the opening, to form the ridge. The space held open in the crack by crushed ice (call it the "cork width") is a random variable, which scaling suggests may be proportional to the ridge-keel depth. When observed along a track, the cork width will be randomized by the orientation distribution. The random variable associated with ridge spacing is, in this case, the sum of two positive random variables, the crack spacing and the cork width. The probability density of ridge spacing, which is calculated as the convolution of the densities of crack spacing and cork width, thus has a limiting value of zero for zero spacing.

Lowry's and Wadhams' method suggests that an exponential model of ridge spacing is reasonable, if the overlap of ridges is taken into account. The alternative approach suggests that the exponential model has problems for small ridge spacing, since due to the cork spacing the ridges tend to be a certain distance apart. For the purpose of calculations in this paper, a uniform distribution of ridges will be assumed, implying an exponential distribution of ridge spacing. It will also be assumed that mean ridge spacing is so large that the effect of ridge overlap is negligible.

1.4 SPECTRAL PARAMETERS OF RIDGED SURFACES

The autocorrelation of a ridged surface can be calculated, based upon the discrete ridge statistics and a specified ridge shape or ensemble of ridge shapes. Coherent scattering-loss formulas and scattering kernels for the incoherent field, based on perturbation techniques, require the autocorrelation as an input. The Fourier transform of the autocorrelation function is the roughness spectrum of the surface. The autocorrelation function and the roughness spectrum are alternative ways of specifying the second moment of the surface. The specification of the second moment is sufficient information to completely characterize a random surface with Gaussian statistics. A ridged surface does not generally have Gaussian statistics and is not completely characterized by the second moment. However, a knowledge of the second moment is often sufficient for predictions of acoustic scattering. In this section, techniques for calculating the spectrum of a ridged surface will be developed, and applied to the example of randomly oriented cylindrical ridges.

The draft of the under-ice surface will be specified by the depth function,

$$\xi = \xi(x) \ ,$$

where x is position. The autocorrelation of the depth is:

$$W(x) = E[\xi(x_1 + x)\ \xi(x_1)]/\sigma^2 \ , \qquad (19)$$

where E[ ] indicates the expected value over all possible realizations of the surface and σ^2 is the variance of the deptn:

$$\sigma^2 = E[\xi(x)^2] \ .$$

It will be assumed from this point that the surface is statistically isotropic so that the autocorrelation depends only on the distance between two points.

The spectrum is the Fourier transform of the autocorrelation. There are one- and two-dimensional spectra associated with one- and two-dimensional transforms of the autocorrelation function. The one-dimensional spectrum, F_1, is

$$F_1(K) = \left(\sigma^2/(2\pi)\right) \int_{-\infty}^{\infty} W(x) \cos(Kx)\, dx \ , \qquad (20)$$

where K is the one-dimensional wavenumber, in the form 2π over wavelength. The two-dimensional transform of the two-dimensional isotropic autocorrelation function reduces to a one-dimensional Hankel transform of the form:

$$F_2(K) = \left(\sigma^2/(2\pi)\right) \int_{0}^{\infty} W(x)\, J_0(Kx)\, K\, dK \ , \qquad (21)$$

where here K is the absolute value of the two-dimensional wavenumber. $F_1(K)$ is defined on the entire real axis, whereas $F_2(K)$ is defined on the positive real axis. Occasionally in the literature, a folded version of $F_1(K)$, defined on the positive real axis, is used. Its value is double that of the original spectrum.

The depth function $\xi(x)$ of a ridged surface is the sum of translates of a given ridge cross-section, $C_j(x)$:

$$\xi(x) = \sum_{j=-N}^{N} C_j(x-x_j) \ . \qquad (22)$$

The ridge cross-section itself may be constant or random. The variable x_j is the position of the j-th ridge.

For the case of a cylindrically shaped ridge of depth h_j and width $R_0 h$, the cross-section is:

$$C_j(x) = \begin{cases} 0 , & x < -h_j R_0, \\ \sqrt{h_j^2 - x^2/R_0^2} , & -h_j R_0 < x < h_j R_0, \\ 0 , & h_j R_0 < x. \end{cases} \qquad (23)$$

When the ridge is crossed at an angle, it will appear wider. The formula for the apparent cross-section of the ridge will be the same as Eq. (23), except that the width-to-height ratio, R_0, is replaced by the apparent ratio, R_j. When the ridges are randomly oriented, the apparent ratio, R_j, has the probability density given in Eq. (14), where R_0, corresponding to W, and R_j, corresponding to W_a, are the width and the apparent width, respectively, of the j-th ridge, measured in units of height, h.

The surface with ridges of elliptical cross-section is interesting for Arctic applications because the asymptotic rate of decay of its roughness spectrum is similar to the large wavenumber behavior of measured ice-roughness spectra. The decay rate is related to the amount of small-scale roughness in the surface. The small-scale roughness associated with an elliptical ridge is concentrated at the corners where the ellipse meets the flat background. It is an open question whether this is an adequate model of the roughness on an ice ridge, or whether the roughness is distributed over the ridge.

The spectrum of a surface with ridges of elliptical cross-section has an asymptotic fall-off of K^{-3}, where K is

the wavenumber, $2\pi/\lambda$, and λ is the wavelength of the roughness in surface. The Fourier transform of the half ellipse, Eq. (22), is a Bessel function which has an asymptotic behavior like $K^{-3/2}$ for large K. The asymptotic behavior of the spectrum is proportional to the square of this,

$$c/K^3 ,$$

with some proportionality factor, c.

The coefficient, c, can be calculated by Fourier transforming the autocorrelation function, W(x), and using the asymptotic properties of the Bessel functions. Based on the definition of the autocorrelation function, Eq. (19), and the stationarity of the process ξ, it follows that:

$$\sigma^2 W(x) = \lim_{N\to\infty} \frac{1}{2N\Delta} \int_{-N\Delta}^{N\Delta} E\left[\xi(t)\ \xi(x+t)\right] dt , \qquad (24)$$

where Δ is the mean spacing between ridges. The spectrum is found by substituting Eq. (24) into Eq. (20), where $\xi(x)$ is defined by Eq. (22). The expression simplifies after interchanging integrals and Fourier transforming the ridge shapes to obtain:

$$F_1(K) = E\left[\lim_{N\to\infty} \frac{1}{2N\Delta} \frac{1}{2\pi} \left| \sum_{j=-N}^{N} \frac{\pi h_j}{K} J_1(Kh_jR_j)\ e^{iKx_j} \right|^2 \right] , \qquad (25)$$

where h_j, R_j, and x_j are the depth, apparent width factor and position of the jth ridge. On carrying out the expected value with respect to ridge position, x_j, the cross terms in the absolute-value-squared factor in Eq. (25) reduce to zero, producing:

$$F_1(K) = E\left[\lim_{N\to\infty} \frac{1}{2N\Delta}\,\frac{1}{2\pi} \sum_{j=-N}^{N} \frac{\pi^2 h_j}{K^2}\, J_1^2(Kh_jR_j)\right] . \qquad (26)$$

On taking the expected value into the sum, Eq. (26) simplifies to:

$$F_1(K) = \frac{\pi}{2\Delta\, K^2}\; E\left[h^2\, J_1^2\,(KhR)\right] . \qquad (27)$$

The asymptotic behavior of Eq. (27) for large K can be found in terms of the asymptotic behavior of J_1^2:

$$J_1^2(z) \sim \frac{1}{\pi z}\,(1 - \sin(2z)). \qquad (28)$$

For large K, the oscillatory part of Eq. (28) makes a negligible contribution to Eq. (27). The asymptotic behavior of the spectrum for large K reduces to:

$$F_1(K) \sim \frac{1}{2\Delta\, K^3}\; E[h]\; E(1/R).$$

When the ridges are randomly oriented, the expected value of 1/R can be calculated using Eq. (14) to be: $\pi/(4\,R_0)$. The spectrum is asymptotic to:

$$F_1(K) \sim \left(\frac{\pi}{8\Delta R_0}\, E(h)\right) \frac{1}{K^3} . \qquad (29)$$

The mean and RMS depth statistics of the surface can be calculated in closed form. The mean depth is:

$$E\left[\xi(x)\right] = E\left[\frac{1}{2N\Delta} \int_{-N\Delta}^{N\Delta} \xi(x)\, dx\right], \qquad (30)$$

where the stationarity of the process $\xi(x)$ has been used. Similarly, the RMS depth is:

$$E\left[\xi^2(x)\right] = E\left[\frac{1}{2N\Delta}\int_{-N\Delta}^{N\Delta}\xi^2(x)\,dx\right]. \tag{31}$$

When Eqs. (22) and (23) are substituted for $\xi(x)$ in Eqs. (30) and (31), the integrals can be carried out to obtain:

$$E\left[\xi(x)\right] = \frac{\pi}{2\Delta}\,E\left[h^2\right]E\left[R\right], \tag{32}$$

and:

$$E\left[\xi^2(x)\right] = \frac{4}{3\Delta}\,E[h^3]\,E[R]. \tag{33}$$

For the case of randomly oriented ridges, the expected value of R is $\pi R_0/2$.

In Eq. (33), it has been assumed that the effect of ridge overlap is negligible.

The statistics of the rough surface depend on the higher moments of the keel-depth distribution. For a Rayleigh distribution of keel depths, the first three moments are:

$$E\left[h\right] = \bar{h}\ , \tag{34}$$

$$E\left[h^2\right] = \frac{4}{\pi}\,\bar{h}^2, \text{ and} \tag{35}$$

$$E\left[h^3\right] = \frac{6}{\pi}\,\bar{h}^3\ . \tag{36}$$

Based on the higher moments of the Rayleigh keel depth distribution, and assuming a random orientation of ridges, the derived statistics of the ridged surface referenced to the bottom of the undeformed level ice, reduce to:

mean ice draft,

$$E(\xi) = \frac{\pi R_0}{\Delta} \bar{h}^2, \tag{37}$$

RMS ice draft,

$$E(\xi^2) = \frac{4R_0}{\Delta} \bar{h}^3, \tag{38}$$

the standard deviation of roughness (the variance of ice draft),

$$\sigma^2 = \frac{4R_0}{\Delta} \bar{h}^3 - \left(\frac{\pi R_0}{\Delta}\right)^2 \bar{h}^4, \text{ and} \tag{39}$$

the asymptotic behavior of the spectrum,

$$F_1(K) \sim \frac{\pi \bar{h}}{8\Delta R_0} \frac{1}{K^3} . \tag{40}$$

Section 2
SAIC INTERIM SCATTERING MODEL/ICE (SISM/ICE)

The SAIC Interim Scattering Model/Ice (SISM/ICE) is a reflection loss model for the coherent reflected field in ice-covered environments. A sequence of scattering-loss formulas based on perturbation techniques provides a smooth transition in frequency to an asymptotic loss level at the highest frequencies. The perturbation formulas are derived in Bass and Fuks[13] and are summarized in Stokes.[14] The derivation of the formula for the asymptotic loss level is contained in Burke and Twersky[15] and is the same one used in Diachok.[1] The probabilistic techniques derived in Section 1 are used to relate the standard deviation of roughness to the ice-roughness parameters required by the individual reflection-loss formulas. The standard deviation of roughness is the only parameter required by the model for predictions. A contour map of the standard deviation of roughness in meters, shown in Figure 1, is from Buck.[16] It is already available to Fleet users as part of Buck's empirical transmission-loss model. The range of validity of SISM/ICE is from 0-5000 Hz and 0-45 degrees.

2.1 ICE ROUGHNESS PARAMETERS

The under-ice surface is considered to be flat with cylindrical bosses of elliptical cross section.

The bosses:

1) have a half-width-to-depth ratio R_0 of 1.6 as suggested by Diachok,[1]
2) have a Rayleigh depth distribution,

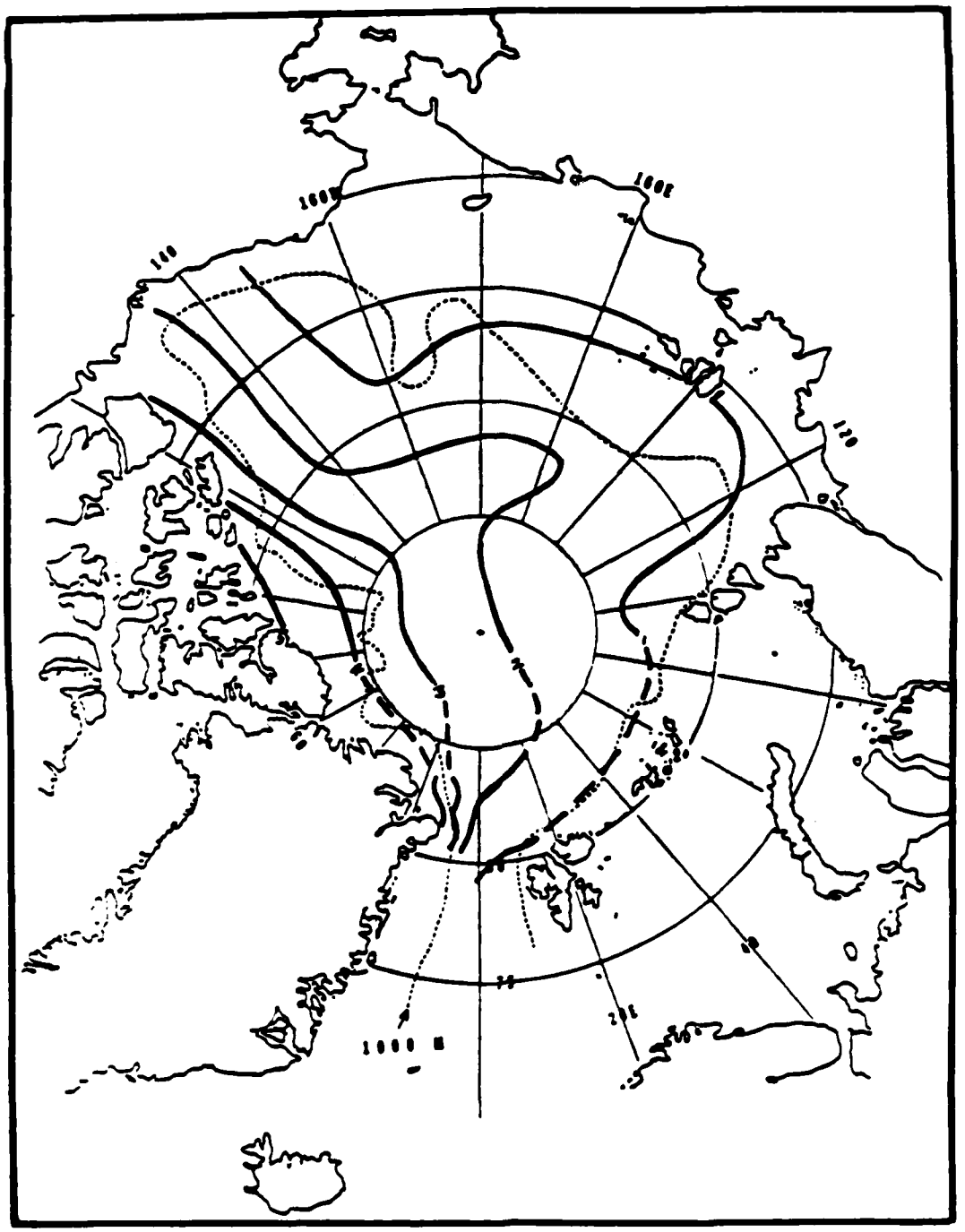

Figure 1. Contours of standard deviation ice depth (m) per LeSchack. Dotted line (...) is 1000 m depth contour and delineates ocean area for which TL models apply.

3) have random orientation, and
4) have random spacing along a track.

Based on these assumptions, the standard deviation of roughness, σ, and the asymptotic behavior of the spectrum are related to the ridge keel parameters by Eqs. (39) and (40), where:

$R_0 = 1.6$ is the half-width-to-depth ratio,
Δ is the mean keel spacing, and
$\bar{h}$ is the mean keel depth.

Under-ice roughness spectra measured along a track can be well approximated by the two-parameter spectral model,

$$\frac{c}{(\beta^2 + K^2)^{3/2}} , \tag{41}$$

where K $(=2\pi/\lambda)$ is the wavenumber of the roughness component in the surface. This function has an asymptotic fall-off for large K of the form:

$$\frac{c}{K^3} . \tag{43}$$

The standard deviation of roughness derived from such a spectrum is:

$$\sigma^2 = \frac{2c}{\beta^2} . \tag{43}$$

2.2 DERIVATION OF ICE-ROUGHNESS PARAMETERS FROM THE STANDARD DEVIATION OF ROUGHNESS

The SISM/ICE model is a hybrid of scattering tneories based on continuous and discrete roughness models. Probabilistic techniques are used to estimate all the required parameters for both types of model, based on the single parameter, the standard deviation of roughness. An assumed random orientation of ridges and effective ridge shape are used to calculate a surface roughness spectrum. Two discrete parameters, the mean ridge spacing and depth, are calculated as inputs to the Burke and Twersky[15] scattering theory.

If the mean ridge spacing is known, the mean keel depth can be estimated from the standard deviation of roughness by solving Eq. (39) as the limit of the following iterative algorithm:

$$\bar{h}_{n+1} = \left[(\Delta/4R_0)(\sigma^2 + \pi^2 R_0^2 \bar{h}_n^4/\Delta^2) \right]^{1/3}. \qquad (44)$$

For the purposes of this model, it is assumed that the mean ridge spacing is:

$$\Delta = 100 \text{ m}.$$

An improved estimate of Δ on a regional basis could be used to improve estimates.

The spectral scattering models, based on the spectral model, Eq. (41), require the two parameters,

$$c = \frac{\pi \bar{h}}{8 \Delta R_0}, \qquad (45)$$

from Eq. (40), and:

$$\beta = (2c/\sigma^2)^{1/2} , \qquad (46)$$

from Eq. (43).

The autocorrelation function related to Eq. (41) is:

$$\beta r \, K_1 (\beta r),$$

where K_1 is a Bessel function of imaginary argument and r is the separation distance. The two-dimensional isotropic roughness spectrum related to Eq. (41) is:

$$\frac{2c}{(\beta^2 + K^2)^2}$$

2.3 REFLECTION LOSS FORMULAS

In terms of the ice-roughness parameters, four formulas for the reflected power $|R^2|$ are evaluated. The predicted value of $|R^2|$ is the maximum of the four calculated values.

- Low Frequency-Free Surface Formula

$$|R|^2 = 1 - 4 (\sin\theta) \, k^2\sigma^2(1-\pi^2 c \, (\sin\theta)/2), \qquad (47a)$$

- High Frequency-Free Surface Formula

$$|R|^2 = 1 - 4 (\sin\theta) \, (1.198) \, c \, (k/\beta)^{3/2} , \qquad (47b)$$

- High Frequency-Rigid Surface Formula

$$|R|^2 = \begin{cases} \dfrac{(\sin\theta - x)^2 + x^2}{(\sin\theta + x)^2 + x^2} & , \; x < \sin\theta \; , \\ .2 & , \; x > \sin\theta \; , \end{cases} \qquad (47c)$$

where:

$$x = 1.311 \; c \; (k/\beta)^{1/2} \; .$$

- Asymptotic Twersky formula

$$|R|^2 = (\sin\theta - x)^2/(\sin\theta + x)^2 \; , \qquad (47d)$$

where:

$$\begin{aligned} x &= n \; L \cos(\theta - \gamma), \\ \tan\gamma &= \rho^{-2}\tan\theta, \\ L^2 &= w^2(\tan^2\theta + \rho^4)/(\tan^2\theta + \rho^2), \\ w &= R_0 \; \pi \; h/2, \\ \rho &= 2/(R_0\pi), \\ n &= 1/\Delta. \end{aligned}$$

In all of formulas 47a-47d, θ is grazing angle and k is the acoustic wavenumber in inverse meters.

2.4 DISCUSSION

SISM/ICE is suggested as an interim scattering-loss model in ice-covered environments. It is based on several simplifications and assumptions. However, it fulfills the requirement for a loss model with a wide range of validity, based on the only known environmental parameter, the standard deviation of roughness. SISM/ICE can be used with acoustic

propagation models such as FACT and RAYMODE to predict the coherent propagating field. However, ray-based models may not adequately reproduce source and receiver depth effects due to modal propagation at the lower frequencies. There may also be a significant incoherent component propagating at the higner frequencies, which would not be predicted by these models. As propagation models become available which can describe the propagating incoherent field, SISM/ICE can be extended to give the scattering kernel for the incoherent field. The details for doing this are contained in Refs. 13, 14, and 15.

Section 3
HIGH-ANGLE PE SIMULATION OF ARCTIC TRANSMISSION LOSS

The High-Angle Parabolic Equation (HAPE) has been used to simulate transmission-loss data reported by Diachok[1], taken at two locations in the Beaufort Sea. The data sets are representative of the Central Arctic environment and the off-shore Canadian environment. The dominant loss mechanism was found to be scattering from Arctic sea-ice ridge keels. For the purpose of the HAPE simulations, equally spaced trapezoidal ridges were used. Two simulated transmission loss runs were carried out at each location, the first with random depth keels, the second with equal sized keels whose depth was equal to the mean depth of the random keels. For both data sets, the random depth keels produced significantly more loss than the constant depth keels, and gave good agreement with the data.

3.1 ENVIRONMENTAL DATA

The random keel depths used in the simulations satisfy the Rayleigh distribution, Eq. (5). This is a one-parameter model, dependent on the mean keel depth. In the Central Arctic case, the mean keel depth and the mean ridge spacing suggested by Diachok[1] were used in the simulation. In the off-shore case, the mean keel depth was estimated from a histogram of ridge-keel depths published by Hibler[2]. These data are based on upward-looking sonar measurements carried out by the USS Sargo in the winter of 1960, near the location of the off-shore transmission-loss experiment. Hibler's data provide statistics for keel depth and mean spacing of ridges deeper than 6.1 meters. The keel-depth distribution for

smaller ridges has been extrapolated, based on a least squares fit of the Rayleigh distribution to the histogram. In addition, the overall mean ridge spacing has been estimated from the published figure, which once again relates to ridges deeper than 6.1 meters, by multiplying by the estimated percentage of ridges deeper than 6.1 meters. The width of the ridges was assumed to be 3.2 times the height, consistent with Diachok.[1] In the HAPE simulations, the ridge width was increased by a factor of $\pi/2$, to account for the mean apparent expansion due to random orientation.

In all simulation runs, the compressional sound speed in the ice was assigned the value 2280 m/s. The density was set at .89 g/cc. The sound speed profile in the water was linearly interpolated in depth between the values in the following table:

depth (m)	speed (m/s)
0.0	1436.0
50.0	1436.0
100.0	1443.0
300.0	1457.8
700.0	1466.6
1085.0	1473.5

A water depth of 1085 meters was used in all simulations. The ocean bottom was assumed to be totally absorbing. In the off-shore case, the measurement tracks lie over shallow ridge and abyssal-hill bottom environments, associated with the Lomonosov ridge and Alpha Cordillera. The bottom loss for the off-shore case can be expected to be quite high. In the Central Arctic case, the measurement tracks lie over the Canada Abyssal Plain, where water depth

averages approximately 3500 meters. The ocean bottom in the abyssal plain environment can be expected to be a good reflector. Buck[18] observes that in the Beaufort Sea, the bottom-reflected energy makes up the major part of the total received energy for ranges up to 55 km.

3.2 ANALYSIS OF DATA AND CONCLUSIONS

The comparison between HAPE simulations and data from the Central Arctic environment is shown in Figures 2 and 3. Trapezoidal ice ridges with a mean depth of 4.3 meters and spacing of 9.5 ridges per kilometer were used. These are the values suggested by Diachok[1], in his analysis of the data. In Figure 2, the ridges have a constant depth and are equally spaced. At both 40 and 50 Hz, the simulation underestimates the observed loss at all ranges. At 300 km, the difference is about 5 dB. In Figure 3, the ridges have a random depth with Rayleigh distribution. The simulation with random depth ridges gives good agreement with the data at long ranges, while overestimating the loss at short ranges. Buck[18] demonstrates convincingly that the differences at the short ranges are due to bottom-reflected energy, which was not included in the simulation. The implications of this numerical experiment for future modeling efforts are:

1) Scattering from random depth ice-ridge keels can account for observed transmission-loss levels in the Arctic.

2) Random depth keels with a Rayleigh depth distribution produce more transmission loss than equal depth keels of the same mean depth.

3) The relevant ridge statistics, mean keel depth and spacing, required for transmission-loss calculations can be estimated from observations.

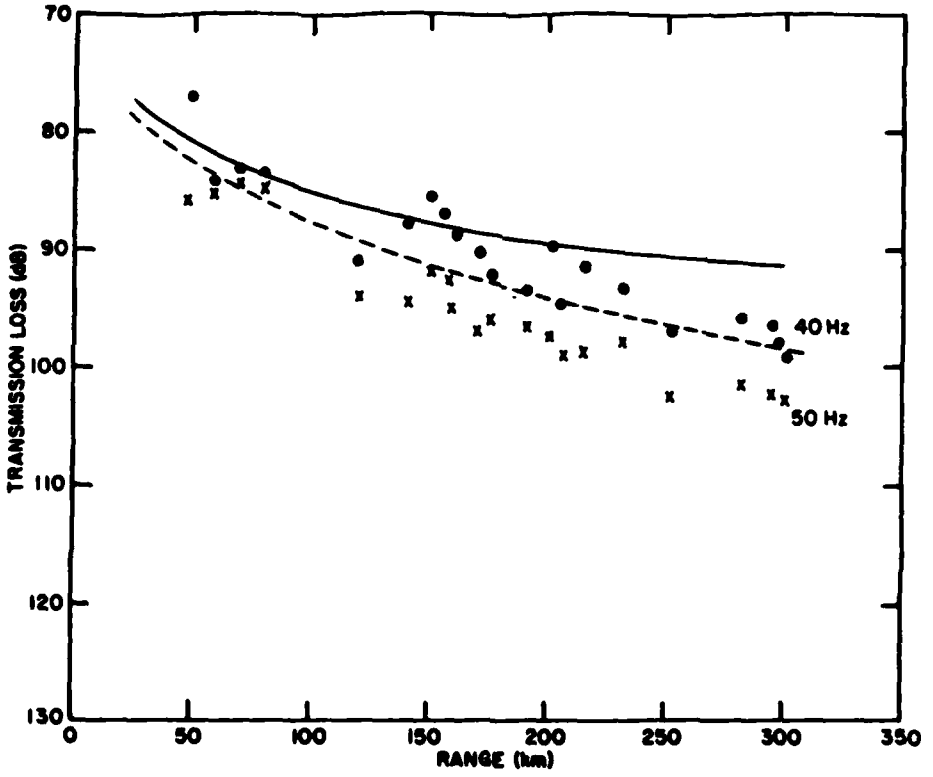

Figure 2. Based on a simulated ice surface consisting of equal depth, equally spaced trapezoidal ice keels, transmission-loss data at the Central Arctic site at 40 Hz (....) and 50 Hz (xxxx) is compared with simulated transmission loss at 40 Hz (———) and 50 Hz (----), using the Arctic High Angle PE.

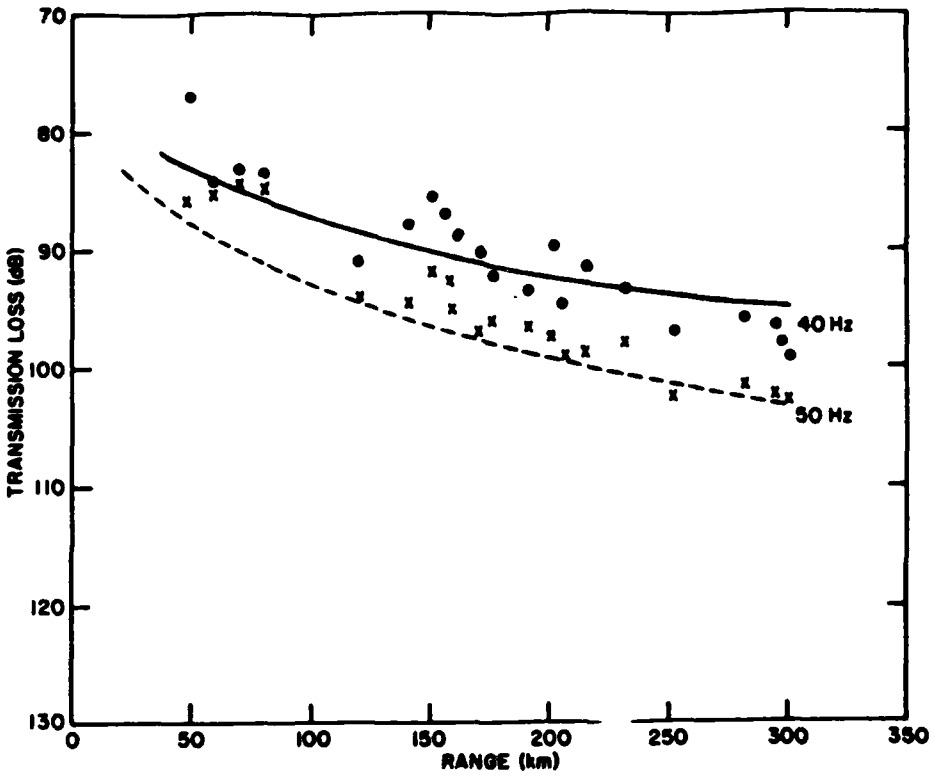

Figure 3. Based on a simulated ice surface consisting of random depth, equally spaced trapezoidal ice keels, transmission-loss data at the Central Arctic site at 40 Hz (....) and 50 Hz (xxxx) is compared with simulated transmission loss at 40 Hz (———) and 50 Hz (----), using the Arctic High Angle PE.

4) Scattering is dominated by the deeper ridges, implying that ridge observations should emphasize the larger ridges.

5) The bottom-bounce path may produce an important contribution at short ranges in an abyssal plain environment.

The transmission-loss data from the measurement tracks in the off-shore Canadian environment are shown in Figure 4 at 40 Hz and Figure 5 at 50 Hz, together with HAPE simulations. A mean keel depth of 7.7 meters and keel spacing of 10 per kilometer were estimated from Hibler's[2] histogram of observed keel depths for the Offshore Province, subprovince 1, located near the middle of the measurement tracks. These keel statistics correspond to a standard deviation of roughness of about 4.5 meters.

In Figures 4 and 5, the solid line corresponds to the simulation results with equal sized ridges, the dashed line to random depth ridges of Rayleigh depth distribution. Once again, the random depth keels produce more loss than the equal depth keels, in this case on the order of 10 dB at a range of 300 km. The random depth simulation mimics the slope of the data extremely well, but underestimates observed loss by a constant 4 dB at 40 Hz and 7 dB at 50 Hz. The 40-Hz data was shifted by 3 dB in an unknown direction as published by Diachok, suggesting that the difference may be 7 dB in both cases.

Despite the differences in level, several conclusions are possible:

1) Random depth keels with a Rayleigh depth distribution produce more transmission loss than equal depth keels of the same mean depth.

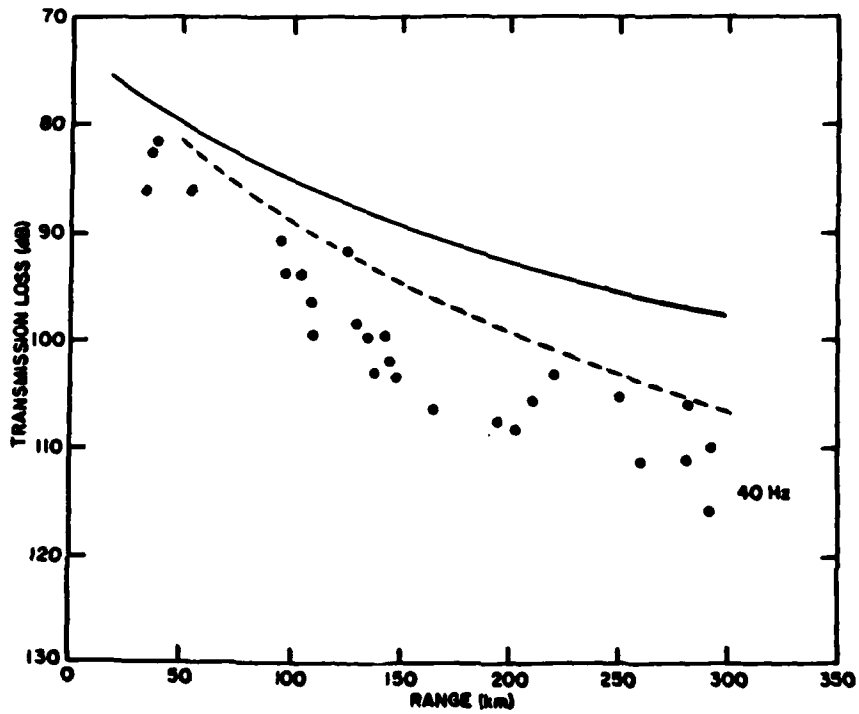

Figure 4. Simulated transmission loss at 40 Hz, using the Arctic High Angle PE, based on a simulated off-shore Canadian ice ridge environment with equal depth, equally spaced trapezoidal keels (————) and random depth, equally spaced trapezoidal keels (----) are compared with 40 Hz transmission-loss data.

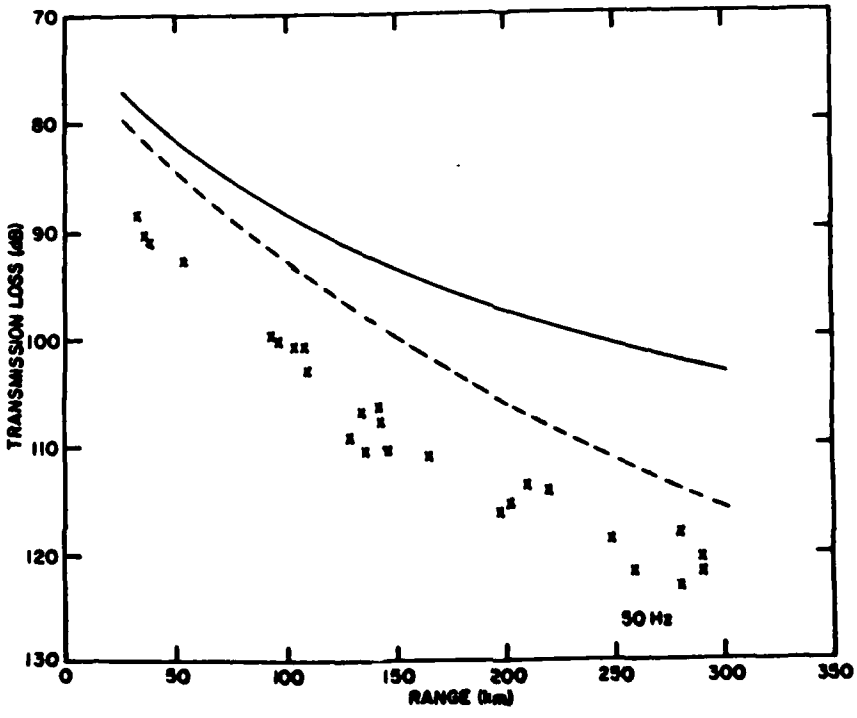

Figure 5. Simulated transmission loss at 50 Hz, using the Arctic High Angle PE, based on a simulated off-shore Canadian ice ridge environment with equal depth, equally spaced trapezoidal keels (———) and random depth, equally spaced trapezoidal keels (----) are compared with 50 Hz transmission-loss data.

2) Scattering from random depth ice-ridge keels with Rayleigh depth distribution can account for the observed rate of decay in range of observed transmission-loss levels in the Arctic.

3) The ridge statistics, mean keel depth and spacing, supporting the transmission-loss calculations can be estimated from observations.

Appendix A

BIBLIOGRAPHY

1. O. I. Diachok, "Effects of sea-ice ridges on sound propagation in the Arctic Ocean," J. Acoust. Soc. Am., 59, 1110-1120 (1976).

2. W. D. Hilber III, W. F. Weeks, and S. J. Mock, "Statistical Aspects of Sea-Ice Ridge Distributions," Journal of Geophysical Research, 77, 5954-5970 (1972).

3. W. D. Hibler III, "Characterization of Cold-Regions Terrain Using Airborne Laser Profilometry," Journal of Glaciology, 15, 329-347 (1975).

4. R. T. Lowry and P. Wadhams, "On the Statistical Distribution of Pressure Ridges in Sea Ice," Journal of Geophysical Research, 84, 2487-2494 (1979).

5. S. J. Mock, A. D. Hartwell, and W. D. Hibler III, "Spatial Aspects of Pressure Ridge Statistics," Journal of Geophysical Research, 77, 5945-5953 (1972).

6. P. Wadhams, "Sea-ice topography of the Arctic Ocean in the region 70°W to 25°E," Philosophical Transactions of the Royal Society of London, 302, 45-85 (1981).

7. S. F. Ackley, W. D. Hibler III, F. K. Kugzruk, A. Kovaks, and W. F. Weeks, "Thickness and Roughness Variations of Arctic Multi-year Sea Ice," AIDJEX Bulletin (1974).

8. W. D. Hibler III and L. A. LeSchack, "Power Specrum Analysis of Undersea and Surface Sea-Ice Profiles," Journal of Glaciology, 11, 345-356 (1972).

9. W. D. Hibler, "Two Dimensional Statistical Analysis of Arctic Sea Ice Ridges," in Sea Ice Conference Proceedings, Reykjavik, 1972.

10. D. A. Rothrock and A. S. Thorndike, "Geometric Properties of the Underside of Sea Ice," Journal of Geophysical Research, 85, 3955-3963 (1980).

11. R. H. Mellen, "Underwater Acoustic Scattering from Arctic Ice," J. Acoust. Soc. Am., 40, 1200-1202 (1966).

12. W. Feller, An Introduction to Probability Theory and Its Applications (John Wiley and Sons, Inc., New York, 1971), 2nd ed., Chap. II, pp. 61-62.

13. F. G. Bass and I. M. Fuks, Wave Scattering from Statistically Rough Surfaces, Pergamon Press, New York (1979).

14. A. P. Stokes, "A Primer on Rough Surface Scattering," Science Applications Inc. Report No. SAI-83-140-WA, 1710 Goodridge Drive, McLean, VA 22102 (April 1983).

15. J. E. Burke and V. Twersky, "Scattering and Reflection by Elliptically Striated Surfaces," J. Acoust. Soc. Am. 40, 883-895 (1966).

16. B. M. Buck, "Preliminary Underice Propagation Models Based on Synoptic Ice Roughness (Area TR No. 9)," Polar Research Laboratory Report TR-30, 123 Santa Barbara St., Santa Barbara, CA 93101 (May 1981).

17. R. R. Greene, "The Rational Approximation to the acoustic wave equation with bottom interaction," to appear J. Acoust. Soc. Am. (1984).

18. B. M. Buck and C. R. Greene, "Arctic Deep-Water Propagation Measurements," J. Acoust. Soc. Am., 36, 1526-1533 (1964).

Appendix B
DISTRIBUTION LIST

ADDRESSEE	DODAAD CODE	NUMBER OF COPIES
Mr. B. Wheatley Code 270 Naval Ocean Research and Development Activity NSTL Station Bay St. Louis, MS 39529	N68462	1
DCASMA San Diego Bldg. 4, AF Plant 19 4297 Pacific Highway San Diego, CA 92110 ATTN: B. J. Clause	S0514A	1
Director, Naval Research Laboratory, ATTN: Code 2627 Washington, D.C. 20375	N00173	6
Naval Ocean Research and Development Activity ATTN: Code 125 NSTL Station, MS 39529	N68462	20

(NORDA Code 125 will provide the required number of copies to Defense Technical Information Center (DTIC))

END

FILMED

3-85

DTIC